Contribution from Lehrstuhl für Theoretische Chemie, Technische Universität München, Lichtenbergstrasse 4, 8046 Garching, Federal Republic of Germany, and Dipartimento di Chimica Inorganica e Metallorganica, Centro CNR, Università di Milano, via Venezian 21, 20133 Milano, Italy

Electronic Structure of Nickel Carbonyl Clusters: Chemical Bonding and Spectroscopy of $[Ni_5(CO)_{12}]^{2-}$, $[Ni_6(CO)_{12}]^{2-}$, and $[Ni_8C(CO)_{16}]^{2-}$ Studied by the LCGTO–LDF Method

Gianfranco Pacchioni*,†,‡ and Notker Rösch*,†

Received January 11, 1990

We report the results of linear combination of Gaussian type orbitals (LCGTO) local density functional (LDF) calculations on the electronic structure of naked and carbonylated Ni clusters. We found substantial differences in the electronic structure and bonding characteristics of the two classes of compounds. In bare Ni clusters the bonding is more metallic, while in the corresponding carbonylated compounds a substantial gap separates the occupied and the virtual levels. As a consequence of carbonylation, the average atomic configuration goes from $3d^94sp$ to (formally) $3d^{10}$, and thus the strength of the metal–metal bond changes. This is supported by the analysis of (a) density of states (molecular orbitals), (b) electron density, and (c) energetics of bare and ligated clusters. These results are discussed in view of the proposed "molecular cluster–surface" analogy. The formation of the dianionic $[Ni_n(CO)_m]^{2-}$ cluster from the corresponding neutral form results in a considerable stabilization. It is shown that, in general, the two extra electrons play an important role in bonding the monomeric units into the oligomeric cluster forms. Finally, the solution optical spectrum of $[Ni_6(CO)_{12}]^{2-}$ is reported and interpreted in terms of one-electron transitions.

1. Introduction

Metal cluster chemistry is one of the most rapidly expanding areas within organometallic chemistry.[1] The largest class is composed of clusters in which the metal atoms are formally zerovalent and the associated ligands have substantial π-acceptor character, as in metal carbonyl clusters. When the first examples of molecular metal clusters were synthesized, the main interest of the chemical community was directed toward their use as potential homogeneous catalysts.[2] Later, it was proposed that discrete molecular metal clusters may represent reasonable models of metal surfaces in processes of chemisorption and heterogeneous catalysis.[3] More recently, organometallic clusters have stimulated the investigations of solid-state physicists interested in the transition of the physical properties of the clusters (in particular the magnetic behavior) to those of bulk materials.[4]

Traditionally performed in solution,[5] or with matrix isolation techniques,[6] the synthesis of gas-phase Ni cluster carbonyls has been recently carried out also in molecular beams.[7]

It is no wonder that this novel class of inorganic compounds has stimulated strong interest and curiosity among theoreticians. Several theoretical and computational studies have been reported with the aim of elucidating the nature of the bonding in these fascinating compounds.[8] However, the understanding of the electronic structure of molecular metal clusters is rather poor and still represents a great challenge to quantum chemists.[8a] The main reasons are the dimensions of the systems and the presence of transition-metal atoms, both of which make it difficult to apply standard ab initio quantum-chemical methods in a routine fashion. Therefore, many simplified procedures have been proposed, including the electron-counting method proposed by Wade[9] on the basis of the analogy with borane chemistry and the model based on extended Hückel theory proposed by Lauher.[10]

Electron-counting schemes try to establish a relationship between the number of valence electrons of a cluster and the nodal characteristics of the metal orbitals; the latter, in turn, depend upon the geometrical structure of the metal framework. Among these theories, the topological electron-counting method, recently proposed by Teo and based on the Euler's theorem,[11b-d] warrants particular attention because it was shown to be quite successful in predicting the number of valence electrons associated with carbonyl clusters. Although such an essentially topological approach is of considerable value in the development of new synthetic routes for cluster species,[11a] it nevertheless does not provide insight into the true nature of the metal–metal and metal–ligand interactions in the cluster. On the other hand, whereas studies performed with approximate computational schemes, mainly extended Hückel,[12] Fenske–Hall,[13] and INDO,[14] have provided qualitative correlations among computed bond orders, density of states, electronic transitions, spin distribution, experimental bond distances, and photoelectron, EPR, and optical spectra etc., more quantitative interpretations of the bonding are scarce, and to date essentially based on chemical potential[15] or discrete variational $X\alpha$[16] investigations.

In this work we present the results of an accurate all-electron study of the electronic structure of $Ni_5(CO)_{12}$, $Ni_6(CO)_{12}$, and $Ni_8C(CO)_{16}$ and of their dianions performed with the linear combination of Gaussian-type orbitals (LCGTO) local density functional (LDF) method.[17] This computational technique, described in section 2, is quite well suited for the study of the transition from magnetic to diamagnetic systems,[18] a central

† Technische Universität München.
‡ Università di Milano.

(1) (a) Moskovits, M., Ed. *Metal Clusters*; Wiley: New York, 1986. (b) Gates, B. C., Guczi, L., Knözinger, H., Eds. *Metal Clusters in Catalysis*; Elsevier: Amsterdam, 1986.
(2) Muetterties, E. L.; Krause, M. J. *Angew. Chem., Int. Ed. Engl.* **1983**, *22*, 135.
(3) Muetterties, E. L.; Rhodin, T. N.; Band, E.; Brucker, C. F.; Pretzer, W. R. *Chem. Rev.* **1979**, *79*, 91.
(4) (a) Johnson, D. C.; Benfield, R. E.; Edwards, P. P.; Nelson, W. H. J.; Vargas, M. D.; *Nature* **1985**, *314*, 231. (b) Pronk, B. J.; Brom, H. B.; de Jongh, L. J.; Longoni, G.; Ceriotti, A. *Solid State Commun.* **1986**, *59*, 349. (c) Teo, B. K.; Di Salvo, F. J.; Waszczak, J. V.; Longoni, G.; Ceriotti, A. *Inorg. Chem.* **1986**, *25*, 2262.
(5) Chini, P. *J. Organomet. Chem.* **1980**, *200*, 37.
(6) Morton, J. R.; Preston, K. F. *Inorg. Chem.* **1985**, *24*, 3317.
(7) Fayet, P.; McGlinchey, M. J.; Woste, L. H. *J. Am. Chem. Soc.* **1987**, *109*, 1733.
(8) (a) Manning, M. C.; Trogler, W. C. *Coord. Chem. Rev.* **1981**; *38*, 89. (b) Pacchioni, G. In *Elemental and Molecular Clusters*; Benedek, G., Martin, T. P., Pacchioni, G., Eds.; Springer: Berlin, 1988.
(9) (a) Wade, K. *J. Chem. Soc., Chem. Commun.* **1971**, 792. (b) Mingos, D. M. P. *Nature* **1971**, *236*, 99. (c) Mingos, D. M. P.; Johnston, R. L. *Struct. Bonding (Berlin)* **1987**, *68*, 29.
(10) Lauher, J. W. *J. Am. Chem. Soc.* **1978**, *100*, 5305. (b) *Ibid.* **1979**, *101*, 2604.
(11) (a) Mingos, D. M. P. *Acc. Chem. Res.* **1984**, *17*, 311. (b) Teo, B. K. *Inorg. Chem.* **1984**, *23*, 1251. (c) *Ibid.* **1985**, *24*, 1627. (d) *Ibid.* **1985**, *24*, 4209.
(12) (a) Dedieu, A.; Hoffmann, R. *J. Am. Chem. Soc.* **1978**, *100*, 2074. (b) Evans, J. *J. Chem. Soc., Dalton Trans.* **1980**, 1005. (c) Evans, D. G.; Mingos, D. M. P. *Organometallics* **1983**, *2*, 435. (d) Halet, J. F.; Hoffmann, R.; Saillard, J. Y. *Inorg. Chem.* **1985**, *24*, 1695. (e) Underwood, D. J.; Hoffmann, R.; Tatsumi, K.; Nakamura, A.; Yamamoto, Y. *J. Am. Chem. Soc.* **1985**, *107*, 5968. (f) Evans, D. G. *Inorg. Chem.* **1986**, *25*, 4602.
(13) Rives, A. B.; Xiao-Zeng, Y.; Fenske, R. F. *Inorg. Chem.* **1982**, *21*, 2286.
(14) (a) Fantucci, P.; Pacchioni, G.; Valenti, V. *Inorg. Chem.* **1984**, *23*, 247. (b) Pacchioni, G.; Fantucci, P. *Chem. Phys. Lett.* **1987**, *134*, 407. (c) Pacchioni, G.; Fantucci, P. *Z. Phys. D* **1989**, *12*, 395.
(15) (a) Chang, K. W.; Woolley, R. G. *J. Phys. C* **1979**, *12*, 2745. (b) Bullet, D. W. *Chem. Phys. Lett.* **1985**, *115*, 450. (c) *Ibid.* **1987**, *135*, 373.
(16) (a) Delley, B.; Manning, M. C.; Ellis, D. E.; Berkowitz, J.; Trogler, W. C. *Inorg. Chem.* **1982**, *21*, 2247. (b) Holland, G. F.; Ellis, D. E.; Trogler, W. C. *J. Chem. Phys.* **1985**, *83*, 3507. (c) Holland, G. F.; Ellis, D. E.; Trogler, W. C. *J. Am. Chem. Soc.* **1986**, *108*, 1884.
(17) Parr, R. G.; Yang, W. *Density Functional Theory of Atoms and Molecules*; Oxford University Press: New York, 1989.

0020-1669/90/1329-2901$02.50/0

problem for the understanding of the modifications induced by the CO ligands on the electronic struture of a metallic cluster (sections 3 and 4). The bonding in the carbonylated clusters has been analyzed in terms of MO theory and with the help of electron density contour maps in section 5. Electronic excitations have been calculated in order to qualitatively interpret the solution visible/UV spectrum of $[Ni_6(CO)_{12}]^{2-}$ (section 6). Some general concepts about the "molecular cluster–surface" analogy will be discussed in section 7 and the results summarized in the last section.

2. Computational Details

In the LCGTO–LDF method one has to solve effective one-electron equations derived in the Kohn–Sham approach to density functional theory[17]

$$[-\tfrac{1}{2}\nabla^2 + v(r)]\,\psi_i(r) = \epsilon_i\,\psi_i(r)$$

where the local potential v comprises the electron–nucleus attraction, the classical interelectronic repulsion from the charge density ρ

$$\rho(r) = \sum n_i|\psi_i(r)|^2$$

and the exchange correlation potential $v_{xc}(r)$, which in the present investigation is taken to be the Xα variant of the LDF approximation

$$v_{xc}(r) = -\tfrac{3}{2}\alpha[(3/\pi)\,\rho(r)]^{1/3}$$

The parameter α is set to 0.7, a value close to the one appropriate for the exchange only, $^2/_3$. A generalization of the formalism to a spin-polarized version is available to describe systems with unpaired electrons.[17,18]

A fundamental characteristic of the LCGTO–LDF approach[18-21] is the use of three Gaussian-type basis sets leading to an approximate N^3 dependence of the number of required integrals and thus to considerable economy for transition-metal systems with respect to standard Hartree–Fock techniques. Besides the familiar orbital basis, two auxiliary basis set are employed, one for the charge density

$$\rho(r) \approx \bar{\rho}(r) = \sum a_i f_i(r)$$

and one for the exchange correlation potential

$$v_{xc}(r) \approx \bar{v}_{xc}(r) = \sum b_i g_i(r)$$

The coefficients a_i are determined variationally by minimizing the Coulomb self-interaction of the difference $\Delta\rho = \rho - \bar{\rho}$. From a least-squares procedure over a moderate-size grid of points, one obtains the expansion coefficients b_i. The three types of basis sets have to be chosen judiciously and well balanced among each other (for a more extensive discussion see refs 21 and 22).

For Ni, a (15s,11p,6d) basis[23] contracted to [9s,5p,3d] was used. The corresponding fitting basis sets were constructed by properly scaling the exponents of the orbital basis.[22] The quality of this basis set (see basis set no. 6 in Table I of ref 21) was considered adequate for the present study, which focused on charge distribution, one-electron energies and fixed cluster geometries. The basis sets for C and O were taken from a previous study;[24] the orbital basis sets were of the type (9s,5p,1d)[25] contracted slightly to [7s,4p,1d].

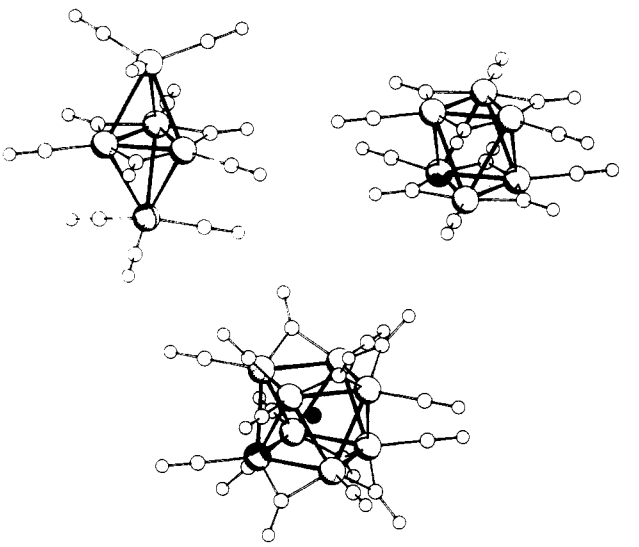

Figure 1. Geometry of the $Ni_n(CO)_n$ clusters considered in this work. The geometrical parameters have been taken from X-ray structures of the corresponding dianions.[30,31]

Table I. Distances, r (Å), Total Energy, E_T (au), Dissociation Energy, D_e (kJ/mol), Fermi Energy, E_F (eV), and Number of Unpaired Electrons per Ni Atom, n_s, of Bare Ni_n Clusters[a]

cluster	r_1, r_2[b]	E_T	D_e/n[c]	E_F	n_s
Ni_3	2.38	−4518.1582	130	−2.93	0.83
Ni_5	2.38, 2.81	−7530.3265	163	−3.17	0.84
Ni_6	2.38, 2.77	−9036.4676	196	−3.47	1.14
Ni_8	2.48, 2.63	−12048.7762	247	−3.54	0.99
Ni_8C	2.48, 2.63	−12086.4177	310	−3.44	0.53

[a] Spin-polarized calculations with FON; E(Ni; ^{3}D $3d^9 4s^1$) = −1506.0030 au; E(C; ^{3}P $2s^2 2p^2$) = −37.3288 au. [b] From X-ray structure of the carbonylated counterparts.[30,31] [c] Dissociation energy computed as $[-E(Ni_n) + nE(Ni)]/n$.

For the naked Ni clusters a high density of states is found near the HOMO. This entails a large number of low-lying excited states, nearly degenerate with the ground state. In order to reduce the computational effort necessary for a proper determination of the ground state, we resorted to a procedure that averages over low-lying one-electron configurations. This approach is implemented as a procedure using fractional occupation numbers (FON)[21,26] where each one-electron energy level is formally broadened by a Gaussian. The fractional occupations are determined self-consistently by filling the resulting density of states (DOS) up to the cluster Fermi energy.

The LCGTO–LDF method described above has been successfully applied to a large variety of systems, ranging from organometallic compounds[27] to metal clusters,[18,21] chemisorption systems,[21,26,28] and localized excitons in ionic crystals.[29]

The geometry of the clusters considered in this work were taken from crystal structures of $[Ni_5(CO)_{12}]^{2-}$, $[Ni_6(CO)_{12}]^{2-}$,[30] and $[Ni_8C(CO)_{12}]^{2-}$[31] (see Figure 1 and Table I for Ni–Ni distances). Idealized D_{3h}, D_{3d}, and D_{4d} symmetries were assumed, on the basis of the following

(18) Dunlap, B. I.; Rösch, N. *J. Chim. Phys.* **1989**, *86*, 671.
(19) Dunlap, B. I.; Connolly, J. W. D.; Sabin, J. R. *J. Chem. Phys.* **1979**, *71*, 3396, 4993.
(20) Dunlap, B. I.; Rösch, N. *Adv. Quantum Chem.*, in press.
(21) Rösch, N.; Knappe, P.; Sandl, P.; Görling, A.; Dunlap, B. I. In *The Challenge of d and f Electrons. Theory and Computation*; Salahub, D. R.; Zerner, M. C., Eds.; ACS Symposium Series 394; American Chemical Society: Washington, DC, 1989; p 180.
(22) Jörg, H.; Rösch, N.; Sabin, J. R.; Dunlap, B. I. *Chem. Phys. Lett.* **1985**, *114*, 529.
(23) (a) Wachters, A. J. H. *J. Chem. Phys.* **1970**, *78*, 1033. (b) Spangler, D.; Wendoloski, I. J.; Dupuis, M.; Chen, M. M. L.; Schaefer, H. J., III. *J. Am. Chem. Soc.* **1981**, *103*, 3985.
(24) (a) Rösch, N.; Jörg, H.; Dunlap, B. I. In *Quantum Chemistry: the Challenge of Transition Metals and Coordination Compounds*; Veillard, A., Ed.; NATO ASI Series C 176; Reidel: Dordrecht, 1986; p 179. (b) Rösch, N.; Jörg, H.; Kotzian, M. *J. Chem. Phys.* **1987**, *86*, 4038.
(25) van Duijneveldt, F. B. IBM Research Report RJ 945; IBM Corp.: Mahopac, NY, 1971.
(26) Rösch, N.; Sandl, P.; Görling, A.; Knappe, P. *Int. J. Quantum Chem.* **1988**, *S22*, 275.
(27) (a) Jörg, H.; Rösch, N. *Chem. Phys. Lett.* **1985**, 120, 359. (b) Rösch, N.; Jörg, H. *J. Chem. Phys.* **1986**, *84*, 5967. (c) Rösch, N.; Kotzian, M.; Jörg, H.; Schröder, H.; Rager, B.; Metev, S. *J. Am. Chem. Soc.* **1986**, *108*, 4238. (d) Knappe, P.; Rösch, N. *J. Organomet. Chem.* **1989**, *359*, C5.
(28) (a) Rösch, N.; Sandl, P.; Knappe, P.; Görling, A.; Dunlap, B. I. *Z. Phys. D* **1989**, *12*, 547. (b) Rösch, N.; Görling, A.; Knappe, P.; Lauber, J. *Vacuum*, in press.
(29) (a) Rösch, N.; Knappe, P.; Dunlap, B. I.; Bertel, E.; Netzer, F. P. *J. Phys. C: Solid State Phys.* **1988**, *21*, 3423. (b) Bertel, E.; Memmel, N.; Jacob, W.; Dose, V.; Netzer, F. P.; Rosina, G.; Rangelov, G.; Astl, G.; Rösch, N.; Knappe, P.; Dunlap, B. I.; Saalfeld, W. *Phys. Rev. B* **1989**, 6087.
(30) (a) Longoni, G.; Chini, P.; Lower, L. D.; Dahl, L. F. *J. Am. Chem. Soc.* **1975**, *97*, 5034. (b) Calabrese, J. C.; Dahl, L. F.; Cavalieri, A.; Chini, P.; Longoni, G.; Martinengo, S. *Ibid.* **1974**, *96*, 2616.
(31) Ceriotti, A.; Longoni, G.; Manassero, M.; Perego, M.; Sansoni, M. *Inorg. Chem.* **1985**, *24*, 117.

distances for Ni–CO and C–O bonds: terminal CO, r(Ni–CO) = 1.90 Å, r(C–O) = 1.13 Å; bridge CO, r(Ni–CO) = 1.75 Å, r(C–O) = 1.17 Å. The geometry of the $Ni_3(CO)_3(\mu\text{-}CO)_3$ cluster, which is not known experimentally, was assumed to be the same as in the corresponding building blocks in the Ni_5 and Ni_6 carbonylated clusters.

3. Bonding in Bare Ni_n Clusters

A thorough study of the bonding in bare Ni_n compounds is outside the scope of this work; in fact, their electronic structure has been recently investigated with both Hartree–Fock[32] and local density techniques.[33] However, the understanding of the basic features of the Ni–Ni bonding in isolated Ni clusters is a necessary prerequisite in order to interpret and analyze the perturbations induced by the CO ligands on the cluster electronic distribution.

The Ni_n clusters here considered have not been optimized; their geometry was taken to be the same as in the metal core of their carbonylated counterparts (Figure 1). Equilateral triangle Ni_3 has been calculated in two different ways, with single, configuration calculations and with the fractional occupation numbers technique described in the previous section. The two calculations provide a complementary view of the bonding in this system. As recently shown by Walch,[32b] in Ni_3 there are several low-lying electronic states characterized by high spin multiplicity. The determination of the ground state is thus a complex problem because of the near degeneracy of many electronic states. However, the most general result, supported also by the present calculations, is that all these low-lying states are quintets originating from the interaction of three Ni atoms in a $3d^94s^1$ configuration. In the D_{3h} geometry, the 4s electrons give rise to a $(4s\ a_1')^2(4s\ e')^1$ configuration; the numerous quintet states arise from the many different ways in which the three 3d holes are localized either in 3dδ or in 3dπ orbitals of the Ni atoms. We found that the lowest configuration is the Jahn–Teller unstable quintet $(8a_1')^2(1a_1'')^1(3a_2')^2(3a_2'')^2(11e')^1(4e'')^2$. The calculation on Ni_3 performed with FONs produces a final MO occupancy that is an average over several states of different spin multiplicity (quintets, triplets, etc.). This explains why, according to this calculation, the average number of unpaired electrons per Ni atom, n_s, is 0.83 and not 1.33 as found by computing single configurations with fixed occupation numbers.

There is no doubt about the magnetic character of the Ni_3 cluster. This is true also for the other Ni_n clusters considered (Table I): n_s ranges from 0.8 for Ni_5 to 1.1 for Ni_6; for Ni_8C it is 0.5 only because of the coupling between the cluster unpaired electrons with those of the central carbon atom. The magnetization calculated for the bare Ni_n clusters, 0.8–1.1 μ_B, is considerably larger than the bulk value, 0.57 μ_B. This is not surprising, however, if one takes into account that some of the intermetallic distances in the Ni_n clusters, 2.7–2.8 Å, are much longer than the Ni–Ni separation in the bulk, 2.49 Å. Calculations performed at the same theoretical level for Ni clusters where the Ni–Ni distances have been fixed at the bulk value exhibit the correct magnetization, 0.6 μ_B.[21]

Analysis of the DOS curves (Figure 2), obtained by broadening the discrete one-electron energy levels with a Gaussian function of fixed half-width = 0.2 eV, confirms that the spin density is essentially confined to the 3d levels and that the 4sp band is only partially filled. All the DOS profiles of the Ni_n clusters considered exhibit a well-defined peak of pure sp character below the d band. Inspection shows that this peak corresponds to the totally symmetric combination of the 4s orbitals with negligible 4p contribution. This bonding orbital is of particular importance for the formation of the Ni–Ni bonds and for the stabilization of the cluster; its role in the carbonylated counterparts will be discussed below. Another characteristic feature of the DOS curves of the bare Ni_n clusters is the high density of one-electron levels immediately above the Fermi energy, a typical sign of developing metallic character (see Fig 2).

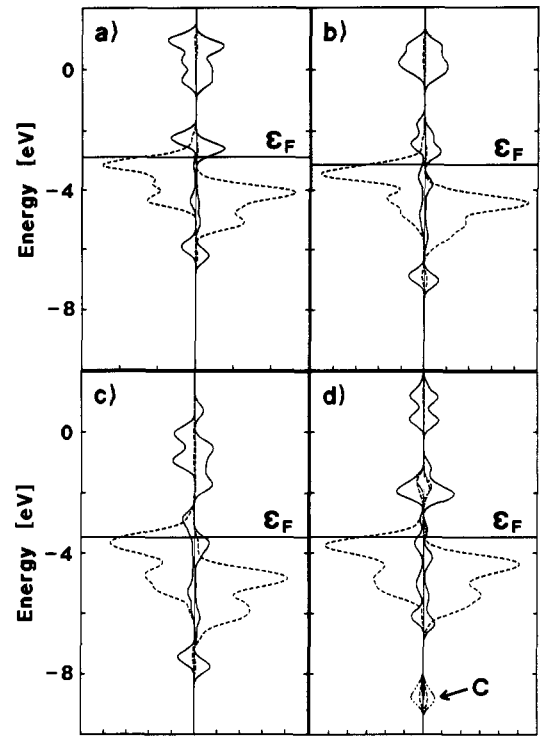

Figure 2. Density of states (in arbitrary units) generated by Gaussian broadening of the one-electron energies (spin-polarized calculation): ---, Ni 3d contribution; —, Ni 4s–4p contribution; (a) Ni_3; (b) Ni_5; (c) Ni_6; (d) Ni_8C; -·-·-, contribution of the C atom. ϵ_F indicates the cluster Fermi energy.

Table II. Total Energy, E_T (au), Dissociation Energy, D_e (kJ/mol), HOMO energy, E_{HOMO} (eV), Number of Unpaired Electrons per Ni Atom, n_s, in Partially and Totally Carbonylated Ni_3 Clusters (Spin-Polarized Calculations)

cluster	E_T	D_e[a]	E_{HOMO}	n_s
Ni_3	−4518.1582		−2.93	0.83
$Ni_3(CO)_3$	−4854.7358	204	−4.00	0.66
$Ni_3(\mu\text{-}CO)_3$	−4854.8542	307	−3.77	0.00
$Ni_3(CO)_3(\mu\text{-}CO)_3$	−5191.4234	252	−4.29	0.00

[a] Dissociation energy determined as $[-E(Ni_3(CO)_n) + E(Ni_3) + nE(CO)]/n$; E(CO, r = 1.127 Å) = −112.1148 au.

To summarize, the present calculations indicate that, in agreement with previous Hartree–Fock[32] and local density[21] studies, the bonding in free gas-phase Ni_n clusters resembles that of the bulk metal; in fact, in both cases the interaction occurs among Ni atoms in a $3d^94s^1$ average configuration. There is also some parallelism between the occupation of the 4s bonding combination in Ni_n clusters and the presence of an occupied 4sp band in the metal. A large, probably dominant, contribution to the bonding in Ni clusters comes from the 4s–4s overlap, while the 3d shells are very localized, with consequent weak coupling of the d electrons. This is the reason for the observed magnetic behavior. This magnetization rapidly converges to the bulk value when bulk distances are considered.[21] As will be shown in the next paragraph, this similarity between clusters and bulk is no longer true when the clusters interact with CO ligands.

4. Consequences of Carbonylation

In order to analyze the electronic structure modifications induced by the addition of the CO ligands to the metal cluster, we consider the cluster model $Ni_3(CO)_3(\mu\text{-}CO)_3$. This system has not been synthesized but represents the building block of higher polymeric forms.[30] The calculations on $Ni_3(CO)_6$ have been done first at the spin-polarized level to see if a residual magnetic moment survives also after the formation of the bond with the carbonyls. The results (see Table II) clearly indicate that the quenching of the Ni_3 magnetism is complete and that the final ground state of $Ni_3(CO)_6$ is diamagnetic. Thus, the presence of six CO ligands

(32) (a) Basch, H.; Newton, M. D.; Moskovitz, J. W. *J. Chem. Phys.* **1980**, *73*, 4492. (b) Walch, S. *Ibid.* **1987**, *86*, 5082.
(33) Lee, K.; Callaway, J.; Kwong, K.; Tang, R.; Ziegler, A. *Phys. Rev. B* **1985**, *31*, 1796.

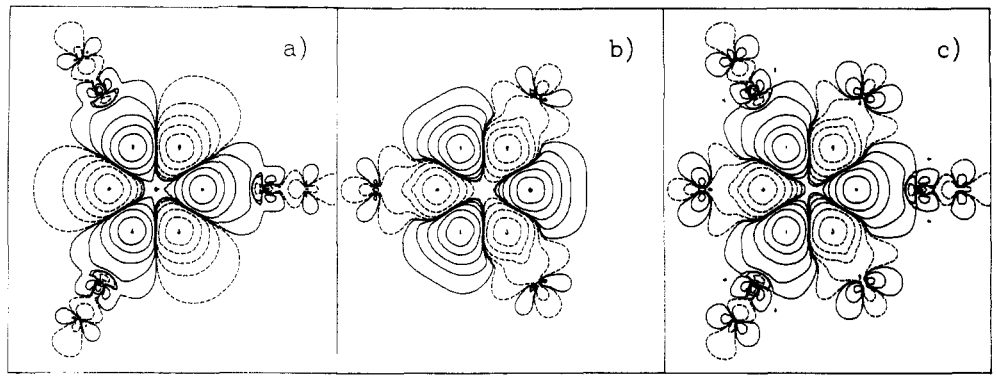

Figure 3. Electron density difference contour maps: (a) $Ni_3(CO)_3$; (b) $Ni_3(\mu\text{-}CO)_3$; (c) $Ni_3(CO)_3(\mu\text{-}CO)_3$. The solid and dotted lines indicate positive and negative values, respectively. The contour lines correspond to 0.001, 0.01, 0.04, 0.2, and 1.0 electron/au^3.

Table III. Total Energy, E_T (au), HOMO and LUMO Energies, E_{HOMO} and E_{LUMO} (eV), and Difference in Stability, ΔE (kJ/mol), for Neutral and Ionic Forms of $Ni_n(CO)_m$ Clusters (Non-Spin-Polarized Calculations)

cluster	E_T	E_{HOMO}, E_{LUMO}	ΔE^a
$Ni_3(CO)_3(\mu\text{-}CO)_3$	−5191.4244	−5.09, −3.55	
$[Ni_3(CO)_3(\mu\text{-}CO)_3]^{2-}$	−5191.3743	+4.94, +6.34	−131
$Ni_5(CO)_9(\mu\text{-}CO)_3$	−8876.7271	−4.55, −4.25	
$[Ni_5(CO)_9(\mu\text{-}CO)_3]^{2-}$	−8876.7742	+3.02, +5.03	+123
$Ni_6(CO)_6(\mu\text{-}CO)_6$	−10382.8696	−5.02, −4.10	
$[Ni_6(CO)_6(\mu\text{-}CO)_6]^{2-}$	−10382.8969	+3.32, +4.75	+71
$Ni_8C(CO)_8(\mu\text{-}CO)_8$	−13881.4393	−4.07, −4.07[b]	
$[Ni_8C(CO)_8(\mu\text{-}CO)_8]^{2-}$	−13881.4995	+2.58, +4.01	+157

[a] Total energy difference between neutral and dianionic species. [b] The highest occupied e_3 MO is occupied by two electrons only and thus coincides with the cluster LUMO.

is sufficient to dramatically change the electron distribution of the Ni_3 fragment.

The most prominent effect is the destabilization of the bonding combination of the Ni 4s orbitals which are now well above the cluster HOMO. The repulsive interaction of the very diffuse 4s-derived MO with the CO 5σ MO is the reason of this destabilization. Consequently, the 4s electrons are excited into the 3d band which becomes completely filled, thus explaining the observed elimination of the original magnetic character. Formally, this corresponds to a change from an atomic $3d^94s^1$ configuration in the bare Ni_n cluster to a $3d^{10}$ configuration in the carbonylated form. Of course, the interaction with the CO ligands induces a strong hybridization of the metal orbitals so that, according to the Mulliken population analysis, the average Ni configuration is $4s^{0.49}4p^{0.38}3d^{8.76}$. The reduction of the 3d population with respect to the formal $3d^{10}$ configuration is mainly due to the large amount of charge back-donation to the CO ligands. A rather similar effective Ni configuration has been found previously in $Ni(CO)_4$.[27a]

A second effect of the carbonylation is the change of the HOMO–LUMO gap, which is extremely tiny in Ni_3 but quite significant in $Ni_3(CO)_6$ (about 1.5 eV, see Table III). In an extended system this would correspond to a metal–insulator transition.

The destabilization of the 4s-derived MO caused by the interaction with the CO ligands, with consequent change in magnetization, is reminiscent of the high-spin to low-spin transition in transition-metal complexes as the consequence of the "field" created by the surrounding ligands. In ligand field theory, if the d-orbital splitting, Δ, exceeds the energy, P, required for electron pairing, a low-spin complex results.[34] The analogy with molecular metal clusters is evident: if number and nature of the ligands destabilize the 4sp-derived orbitals to such an extent that 4s → 3d transitions occur, the resulting molecular cluster will have a diamagnetic or weakly magnetic ground state. It is difficult to establish a scale of increasing field strength generated by a ligand similar to what has been done for transition-metal complexes[35] because of the small variety of ligands involved in the bonding with zerovalent metal clusters (CO, PR_3, PF_3, CNR, olefins). However, as a general rule the most efficient ligands in the magnetic quenching are those ligands which give rise to a strong repulsive interaction in the σ space, e.g. the CO molecule.[36] A similar effect has been found for adsorbates on surfaces.[21,37] Not only the nature of the ligand but also its bonding position (μ_2-bridge, μ_3-bridge, terminal, semibridge, etc.) have a different effect on the magnetic quenching. Indeed, our calculations show that bridging CO ligands are more efficient in reducing the magnetic moment of the Ni atoms than the terminal ones (see Table III) as already found on the basis of simpler calculations.[14b,16b] In $Ni_3(CO)_3$ with three terminal carbonyls, there are still two unpaired electrons in the cluster, while in $Ni_3(\mu\text{-}CO)_3$ the quenching is complete.

All these results provide strong evidence that substantial changes in the Ni–Ni bonds are induced through the interaction with the CO ligands. The reduced 4s participation to the metal–metal bonding of the carbonylated system indicates a decrease of the metal–metal bond strength. This agrees with the recent suggestion that a CO molecule at the bridge site of a Ni_2 molecule causes the breaking of the Ni–Ni bond.[38] In general, however, it is difficult to obtain a simple measure for this bond weakening, which is usually analyzed in terms of bonding or antibonding character of the occupied MOs. One alternative is provided by the analysis of the electron density difference maps (EDDM), obtained by subtracting the electron density of the fragments from that of the whole molecule. Specifically, we have subtracted the superimposed electron densities of the free Ni_3 and CO fragments from those of $Ni_3(CO)_3$, $Ni_3(\mu\text{-}CO)_3$, and $Ni_3(CO)_3(\mu\text{-}CO)_3$ clusters, respectively (Figure 3). The most important effect is already evident from the analysis of the EDDMs for $Ni_3(CO)_3$ and $Ni_3(\mu\text{-}CO)_3$: charge density is accumulated around the Ni centers but depleted between the Ni atoms. A similar picture is found for $Ni_3(CO)_3(\mu\text{-}CO)_3$; the carbonylation has the effect of decreasing the electron density in the Ni–Ni bonding region and of moving charge from the center of the Ni_3 triangle toward the CO ligands.

5. Electronic Structure of Nickel Cluster Carbonyls

The general trends that emerged from the study of the hypothetical $Ni_3(CO)_3(\mu\text{-}CO)_3$ cluster are found also for the higher homologues of the series. In the DOS curves, at lower energies are the CO derived MO levels well separated from the d band, which has a width of about 2.5 eV (see Figure 4). The gap between these two groups of orbitals is about 2–2.5 eV. The Ni 4s-derived MOs are unoccupied, thus confirming the change in

(34) Ballhausen, C. J. *Ligand Field Theory*; McGraw-Hill: New York, 1962.
(35) Jørgensen, C. K. *Absorption Spectra and Chemical Bonding in Complexes*; Pergamon: Elmsford, NY, 1962.
(36) Bagus, P. S.; Nelin, C. J.; Bauschlicher, C. W. *Phys. Rev. B* **1983**, *28*, 5423.
(37) (a) Raatz, F.; Salahub, D. R. *Surf. Sci.* **1986**, *176*, 219. (b) Bauschlicher, C. W.; Nelin, C. J. *Chem. Phys.* **1986**, *108*, 275.
(38) (a) Blomberg, M. R. A.; Lebrilla, C. B.; Siegbahn, P. E. M. *Chem. Phys. Lett.* **1988**, *150*, 522. (b) Siegbahn, P. E. M. Personal communication.

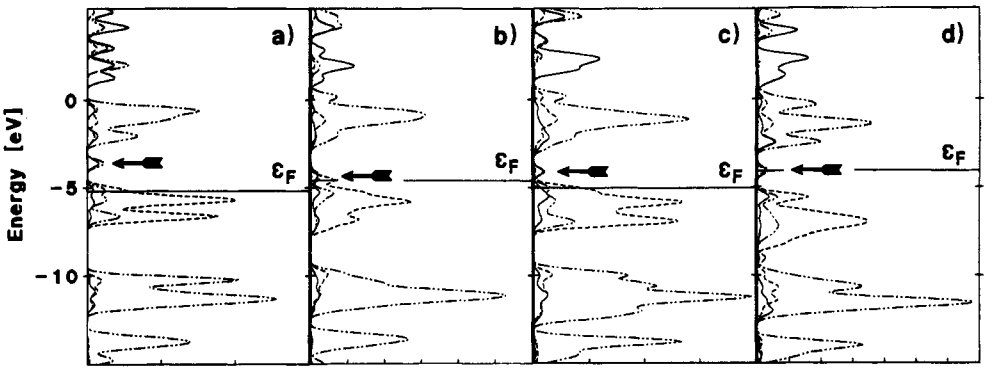

Figure 4. Density of states (in arbitrary units) generated by Gaussian broadening of the one-electron energies (non-spin-polarized calculation): ---, Ni 3d contribution; —, Ni 4s–4p contribution; -···-, contribution of the CO orbitals; (a) $Ni_3(CO)_6$; (b) $Ni_5(CO)_{12}$; (c) $Ni_6(CO)_{12}$; (d) $Ni_8(CO)_{16}$. ϵ_F indicates the cluster Fermi energy (the cluster HOMO). The position of the cluster LUMO is indicated by the arrow.

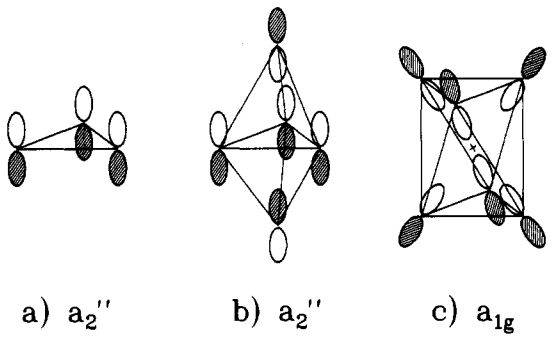

Figure 5. Schematic representation of the unoccupied frontier orbitals in (a) $Ni_3(CO)_6$, (b) $Ni_5(CO)_{12}$, and (c) $Ni_6(CO)_{12}$. Only the metallic atomic orbitals are given.

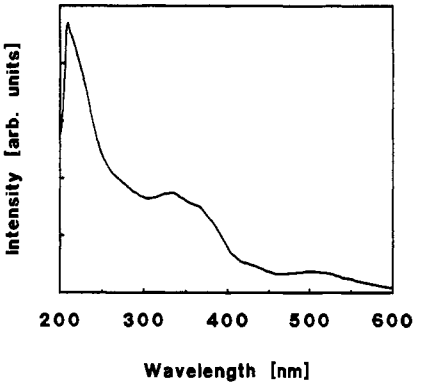

Figure 6. Experimental optical spectrum of $[Ni_6(CO)_{12}]^{2-}$.

electronic configuration of the Ni atoms described in the previous paragraph.

It is worth noting that in all the neutral clusters considered there is a single empty MO slightly above the cluster HOMO. The fact that the LUMO is close to the cluster HOMO, but is much lower in energy than the rest of the unoccupied MOs, suggests that this unoccupied level is likely to act as an "acceptor" of charge and that the cluster electron affinity is small or even positive. In $Ni_8C(CO)_{16}$ this special orbital coincides with the cluster HOMO, which is a degenerate e_3 MO occupied by two electrons only.

The character of these low-lying empty orbitals turns out to be of great importance for the understanding of the formation of the dianion and, eventually, for the oligomerization process. In $Ni_5(CO)_{12}$ the cluster LUMO belongs to a_2'' symmetry and is composed of Ni and CO p_z orbitals (see Figure 5); it has bonding character between the apical $Ni(CO)_3$ units and the basal $Ni_3(CO)_6$ plane. In $Ni_6(CO)_{12}$ the "acceptor" orbital belongs to a_{1g} symmetry; it is a bonding combination of Ni p orbitals oriented toward the center of the triangular antiprism Ni core (see Figure 5). This orbital, once occupied, will contribute significantly to the bonding between the two $Ni_3(CO)_6$ monomers. In $Ni_8C(CO)_{16}$ the partially filled e_3 MO is a mixture of p_z, d_{xz}, and d_{yz} orbitals with bonding character between the central C atom and the two $Ni_4(CO)_8$ subunits. Again, the addition of two electrons in this MO is expected to increase the bonding between the two $Ni_4(CO)_8$ fragments.

The calculations performed for the dianions confirm this simple qualitative MO analysis. A substantial stabilization of the whole structure arises from the occupation of the previously described empty orbitals in $Ni_5(CO)_{12}$, $Ni_6(CO)_{12}$, and $Ni_8C(CO)_{16}$ clusters (Table III). The formation of the dianion is thus a favorable process as shown by the positive values of the electron affinities of the three systems. The only exception is provided by the "monomer" $Ni_3(CO)_6$. Here, as shown by other studies,[12b,15b] the cluster LUMO is an a_2'' bonding combination of Ni and CO p_z orbital lying about 1.5 eV above the cluster HOMO (Figure 5). In this case, the addition of two electrons to form the $[Ni_3(CO)_6]^{2-}$ species is unfavorable; the excess of negative charge, which in the larger clusters acts as a "glue" between the different fragments, cannot be delocalized over a sufficient number of metal centers and of CO ligands, thus increasing the Coulomb repulsion and destabilizing the structure.

The importance of the two extra electrons for the oligomerization process is well demonstrated by the energetics of the reactions

$$2Ni_3(CO)_6 \rightarrow Ni_6(CO)_{12} \qquad \Delta E = -55 \text{ kJ/mol}$$

$$2Ni_3(CO)_6 + 2e^- \rightarrow [Ni(CO)_{12}]^{2-} \qquad \Delta E = -126 \text{ kJ/mol}$$

It is worth noting that the dimerization of Ni_3 to give the triangular antiprism Ni_6 cluster is accompanied by a large energy gain:

$$2Ni_3 \rightarrow Ni_6 \qquad \Delta E = -396 \text{ kJ/mol}$$

Hence, the bonding between the two neutral Ni_3 fragments is much stronger than the bonding between the two $Ni_3(CO)_6$ units in $Ni_6(CO)_{12}$, consistent with the existence of a weak Ni–Ni interaction in the carbonylated forms. Therefore, the two additional electrons seem to be essential for the stabilization of the ligated complex.

6. Optical Spectra

The optical UV–visible spectrum of $(TBA)_2[Ni_6(CO)_{12}]$ (TBA = tetrabutylammonium) exhibits pronounced peaks at 210, 330, and 504 nm, with shoulders at 240, 370, and 425 nm (see Figure 6). The electronic ground state of the dianion $[Ni_6(CO)_{12}]^{2-}$ belongs to the totally symmetric A_{1g} representation of the D_{3d} symmetry group; hence, exited states in idealized D_{3d} symmetry connected to the ground state by fully allowed electric dipole transitions must belong to the same symmetry of one of the x,y, or z components of the dipole moment, i.e. either to A_{2u} (z) or to E_u (x,y) representations.

Electronic configurations contributing to the spin-allowed $^1A_{2u}$ or ^1E_u excited states are constructed by promoting one electron from an occupied into an unoccupied orbital in such a way that the direct product of the representations of the two involved orbitals exhibits a component belonging to A_{2u} or E_u symmetry. In principle, excitation energies must be computed as the difference

Table IV. Energy and Character of the One-Electron Levels in $[Ni_6(CO)_{12}]^{2-}$ (HOMO Energy as Zero Reference)

orbital	energy, eV	composition, % Ni 4sp	Ni 3d	CO
	Unoccupied Orbitals			
33 e_g	5.05	96	1	3
33 e_u	4.76	97	0	3
25 a_{1g}	4.61	98	1	1
25 a_{2u}	4.57	98	1	1
32 e_g	4.31	3	21	76
32 e_u	3.56	11	28	61
24 a_{2u}	3.34	0	12	88
8 a_{2g}	3.02	1	2	97
31 e_g	2.95	4	36	60
31 e_u	2.78	2	14	72
8 a_{1u}	2.59	0	1	99
24 a_{1g}	2.52	0	5	95
30 e_u	2.35	1	17	82
30 e_g	2.34	3	6	91
29 e_g	2.11	15	6	79
23 a_{2u}	1.95	20	7	73
29 e_u	1.82	24	16	60
7 a_{2g}	1.74	21	5	74
7 a_{1u}	1.44	25	13	62
	Occupied Orbitals			
23 a_{1g}	0.00	46	5	49
28 e_u	−0.91	10	58	32
28 e_g	−1.12	7	87	6
22 a_{2u}	−1.32	31	58	11
27 e_g	−1.51	12	51	27
6 a_{2g}	−1.62	1	97	2
6 a_{1u}	−1.72	1	90	9
5 a_{2g}	−1.74	2	92	6
27 e_u	−1.79	1	89	10
26 e_g	−1.82	3	80	17
26 e_u	−2.12	3	77	20
21 a_{2u}	−2.27	11	73	16
5 a_{1u}	−2.32	2	97	1
22 a_{1g}	−2.47	8	89	3
21 a_{1g}	−2.70	6	71	23
25 e_g	−2.75	2	73	25
20 a_{2u}	−2.76	8	78	14
25 e_u	−2.81	6	75	19
24 e_g	−2.92	1	78	21
24 e_u	−3.00	1	76	23
20 a_{1g}	−3.99	20	70	10

between the total energies of two electronic configurations (ΔSCF) accounting for the orbital relaxation effects that occur upon excitation. Unfortunately, this would require evaluating a very large number of configurations, a procedure quite costly in practice. The method followed here for the determination of the excitation energies consists in the subtraction of the ground state one-electron energy levels (Table IV), a method which cannot be fully justified theoretically but which has been successfully applied, in combination with the local density approximation, to the interpretation of the optical spectra of other inorganic compounds.[16] Experience from applying Slater's transition-state method[17] to excitation energies shows that orbital energy differences provide a crude approximation if the spatial characteristics of the two orbitals involved are similar.

Considering the selection rules described above, the following transitions yield excited configurations of appropriate symmetry for fully allowed electric dipole transitions:

$$a_{1g} \leftrightarrow a_{2u}, e_u \qquad a_{2g} \leftrightarrow a_{1u}, e_u \qquad e_g \leftrightarrow a_{1u}, a_{2u}, e_u$$

Even if one takes into account only transitions in the energy range between 1.8 eV, the lowest excitation, and 6.5 eV, the limit of the experimental spectrum, one finds 116 allowed transitions. Whereas the assignment of the lowest transitions of the spectrum, in the region between 1.8 and 3 eV, is possible, the number of electronic excitations in the range between 3 and 6.5 eV is so large that one is forced to interpret the observed absorption band as an envelope of many electronic transitions of very similar energy. In addition, it has to be considered that the true symmetry of the cluster is lower than D_{3d} so that the dipole selection rules are weak restrictions. Finally, numerous vibronically allowed transitions, not considered here explicitly, may also contribute to the shape of the optical spectrum.

Table V. Dipole-Allowed Transitions (eV) in $[Ni_6(CO)_{12}]^{2-}$

transition	calc	obs (λ, nm)	extinction	assgnt[a]
23 $a_{1g} \rightarrow$ 29 e_u	1.82			Ni 4 sp → 2π*
23 $a_{1g} \rightarrow$ 23 a_{2u}	1.95			
23 $a_{1g} \rightarrow$ 30 e_u	2.35			
28 $e_g \rightarrow$ 7 a_{1u}	2.56	2.45 (504)	5×10^3	Ni 3d* → 2π*
28 $e_u \rightarrow$ 7 a_{2g}	2.65			
23 $a_{1g} \rightarrow$ 31 e_u	2.78			
28 $e_u \rightarrow$ 7 a_{1u}	2.85			
28 $e_u \rightarrow$ 29 e_g	3.02	2.90 (425)	shoulder	Ni 3d* → 2π*
6 $a_{2g} \rightarrow$ 7 a_{1u}	3.06			
28 $e_g \rightarrow$ 23 a_{2u}	3.07			
several transitions		3.33 (370)	shoulder	Ni 3d* → 2π*
several transitions		3.74 (330)	3×10^4	Ni 3d* → 2π*
several transitions		5.36 (240)	shoulder	Ni 3d → 2π*
several transitions		5.88 (210)	7×10^4	Ni 3d → 2π*

[a] 3d and 3d* indicate bonding and antibonding combinations of metal orbitals, respectively (see text).

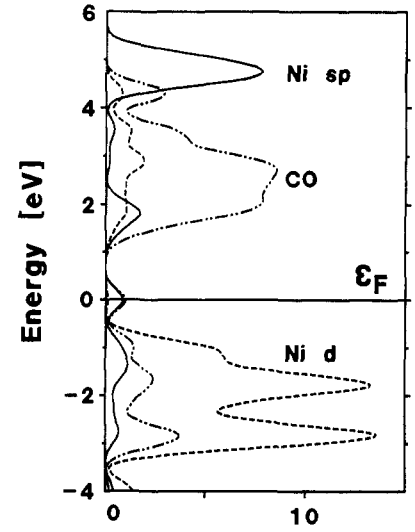

Figure 7. $[Ni_6(CO)_{12}]^{2-}$ density of states (in arbitrary units) generated by Gaussian broadening of the one-electron energies (non-spin-polarized calculation): ---, Ni 3d contribution; —, Ni 4s–4p contribution; -·-·-, contribution of the CO orbitals. ϵ_F indicates the cluster Fermi energy (the cluster HOMO), which is taken as the zero reference energy.

Nevertheless, a rough, purely qualitative, analysis of the spectrum may be attempted on the basis of the present results. The lowest dipole-allowed transitions are calculated at 1.8–1.9 eV, about 670 nm, where the compound starts to adsorb. These transitions (Table V) occur between the cluster HOMO, a combination of 4sp Ni and CO orbitals with negligible 3d character, and the lowest combinations of the CO 2π* MOs. Energetically, the next higher transitions are of 3d → 2π* character, clustering around 2.5 eV (Table V) and corresponding quite well to the first peak in the experimental spectrum. The shoulder observed at 425 nm, about 2.9 eV, can be attributed to a second group of 3d → 2π* transitions centered around 3 eV (Table V). Going to shorter wavelengths, the spectrum exhibits a wide broadening and an increase in the absorption intensity (Figure 6).

The interpretation must remain very qualitative at this point. This part of the spectrum probably originates from several 3d → 2π* transitions. However, if one looks more carefully at the DOS curve of $[Ni_6(CO)_{12}]^{2-}$ (see Figure 7) and at the data of Table IV, it is possible to distinguish, in agreement with other electronic structure calculations of molecular metal clusters,[15,39] a splitting

(39) (a) Drake, S. R.; Johnson, B. F.; Lewis, J.; Woolley, R. G. *Inorg. Chem.* **1987**, *26*, 3952. (b) Woolley, R. G. *Chem. Phys. Lett.* **1988**, *143*, 145.

of the d levels into two bands. These can be roughly classified as metal–metal bonding (M–M) and metal–metal antibonding (M–M*) combinations. The region of the optical spectrum between 2.5 and 5 eV is mainly due to excitations from the top M–M* 3d levels into CO $2\pi^*$ orbitals, while the transitions involving the M–M bonding orbitals in the lower part of the d band and the empty $2\pi^*$ levels may be responsible for the strong feature observed at 210 nm (about 5.9 eV). Finally, it is worth noting that, immediately above this region of the spectrum, around 6.5 eV, a significant number of transitions from the 3d M–M* occupied levels into the empty combinations of Ni 4sp orbitals should occur (Table IV). These transitions, however, are not expected to carry much intensity since they involve much smaller changes in the electronic distribution compared to 3d → CO $2\pi^*$ excitations.

7. The Cluster–Surface Analogy

Molecular fragments bound to metal surfaces display a stereochemistry, and sometimes spectroscopic properties, that very often have precedents in molecular cluster chemistry. This has led to the formulation of the so-called cluster–surface analogy,[3] which is based on the reasonable assumption that the coordination of molecules, radicals, or ions to metal atoms at a metal surface bears some formal analogy to the coordination of these species to one or more metal atoms in discrete molecular complexes, especially in the context of structural features. However, this analogy completely disappears when the reactivity of the two systems is considered: whereas catalysis at metal surfaces represents a broad area of research, few examples of reactions catalyzed by metal clusters have been reported.[2]

What is the main difference between these types of systems? A first more technical observation is that while in crystalline metal surfaces the electronic structure may be described in terms of band theory, in clusters it is more appropriately viewed in terms of molecular orbitals. However, for bare transition-metal clusters of even modest size, e.g. 20 atoms or more, the one-electron-level spectrum begins to approach the bulk DOS.[40] Some, although not all, of the cluster electronic properties converge reasonably rapidly to the bulk values (in particular, cohesive energy, work function, and bond distances).[41] Yet, there is no evidence that large molecular metal clusters, containing 30–40 metal atoms, exhibit a reactivity comparable to that of a metal surface.

Thus, the number of metal atoms is not a key factor differentiating a ligated cluster from a surface. What determines the very different chemical behavior is the presence of the ligands in the molecular clusters, i.e. the nature of nearest neighbors of a reference metal atom. There is enough evidence that, at least qualitatively, metal surfaces and molecular clusters appear to be similar with respect to the nature of the metal–ligand bond, which can be usually described in the same terms (σ donation, π back-donation, etc.). The main quantitative differences lie in the amount of charge transfer and the polarization of the metal moiety. Both are expected to be larger for a molecule chemisorbed at a metal surface than for an additional ligand on a molecular cluster.

As a pictorial, although imperfect, model for these differences, one may compare the EDDMs computed for a single CO molecule on Ni_3, a simple model of on-top and bridge chemisorption on a Ni surface (see Figure 8), with the EDDMs of $Ni_3(CO)_3$ and $Ni_3(\mu\text{-}CO)_3$ clusters (see Figure 3). The electron redistribution in the two types of systems looks very different just because the large metal polarization of the Ni_3 unit in Ni_3–CO is practically absent, for symmetry reasons, in the carbonylated clusters. Whereas on a Ni surface the metal electrons polarize away from the CO 5σ MO, a mechanism that substantially contributes to the bond formation,[36] in molecular metal clusters the electrons

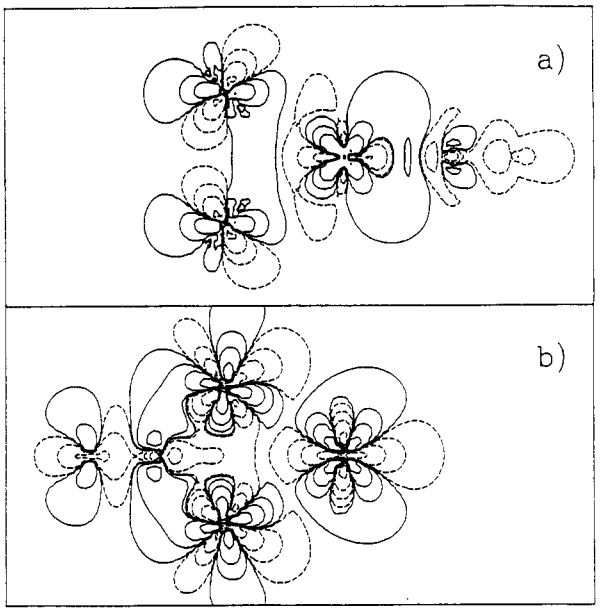

Figure 8. Electron density difference contour maps of $Ni_3(CO)$: (a) terminal CO; (b) bridge CO. The solid and dotted lines indicate positive and negative values, respectively. The contour lines correspond to 0.001, 0.01, 0.04, 0.2, and 1.0 electron/au^3.

seem to flow from the center toward the external region of the metal frame (Figure 3).

The other important difference between molecular clusters and surfaces is that while the magnetic moment in a coordinatively saturated cluster is completely quenched, on metal surfaces, or in their cluster representation, the quenching occurs locally at the chemisorption site while the rest of the material retains its magnetic characteristics.[21,37]

In other words, the main difference between the molecular cluster and the surface regimes is not, or not only, the number of metal atoms, but the very different average coordination of the metal atoms, in both number and kind. The ratio of ligands and metal atoms in molecular clusters is always larger than 1 and very often close to 2 or 3. Even the largest zerovalent cluster compound characterized in the solid state, $[Ni_{38}Pt_6(CO)_{44}]^{2-}$,[42] has one CO ligand per metal atom. On the other hand, on a metal surface, even at high coverage, the metal atoms directly bound to a chemisorbed molecule represent a very small fraction of the effective number of metal atoms in the surface system.

On the basis of the present analysis, it is possible to speculate that, in order to increase the chemical reactivity of molecular clusters, there are in principle two ways. It has been shown,[14b,16b] that, as a consequence of a partial decarbonylation of the cluster, unpaired electrons localized on the coordinatively unsaturated metal atoms may appear. These exposed atoms are probably much more reactive than the other coordinated metal atoms and are potentially the sites where the catalytic reactions occur. This is possibly what happens in catalysis by supported metal clusters.[1b,43] By effect of the interaction with the oxide substrate or by thermal or photochemical treatment, the cluster loses some of the ligands, possibly reconstructs, and eventually dissociates with formation of exposed, very reactive, unsaturated metal fragments. The second obvious way to enhance the molecular cluster reactivity is to increase their size to such an extent that the surface/bulk atom ratio is in favor of the latter. In this case, the change in electronic properties caused by the interaction with ligands will not significantly affect the expected metallic character of the metal particle.

The present discussion has shown that the cluster–surface analogy may be used only in a restricted sense. This analogy has

(40) Heine, V. In *Solid State Physics*; Ehrenreich, H., Seitz, F., Turnbull, D., Eds.; Academic Press: London, 1980; Vol. 35, p 1, and references therein.
(41) (a) Pacchioni, G.; Plavsic, D.; Koutecký, J. *Ber. Bunsen-Ges. Phys. Chem.* **1983**, *87*, 503. (b) Koutecký, J.; Fantucci, P. *Chem. Rev.* **1986**, *86*, 539 and references therein.
(42) Ceriotti, A.; Demartin, F.; Longoni, G.; Manassero, M.; Marchionna, M.; Piva, G.; Sansoni, M. *Angew. Chem., Int. Ed. Engl.* **1983**, *22*, 135.
(43) Lamb, H. H.; Gates, B. C.; Knözinger, H. *Angew. Chem., Int. Ed. Engl.* **1988**, *27*, 1127.

another, yet related dimension: the chemisorption cluster models used successfully in quantum-chemical investigations of chemisorption systems.[21,26,28,37,44] There, a cluster is used to model a finite part of a substrate. Obviously, such model clusters should have a reasonable size in order to provide realistic models of chemisorption sites. Most of the studies so far have analyzed the adsorbate–substrate bond; very few attempts have been undertaken to investigate the much more demanding problem of reactivity.

From past experience and the findings of the present work, a few comments on the use of cluster models seem in order. Typical ligands, such as carbonyl groups, provide a much stronger interaction with the nearest metal atoms than additional surrounding metal atoms. Their effects, such as the polarization of the substrate, may be exaggerated if the substrate model is not large enough (see Figure 8). But the environment of a substrate metal atom, which consists essentially of other atoms of its kind, is certainly very different from that of an atom in a molecular cluster, where a large number of strongly interacting ligands is present. Therefore, the discussion on the limited value of the cluster–surface analogy is not meant to reduce the value of chemisorption model cluster studies. Nevertheless, it is well-known that proper embedding of such chemisorption clusters is highly desirable in order to improve the reliability of their results.[45] Embedding in a truely two-dimensional model of a surface is difficult to achieve. Therefore, attempts to use larger chemisorption cluster models should provide a meaningful route to studying chemisorption.

8. Conclusions

We have performed LCGTO–LDF calculations on the electronic structure of nickel carbonyl clusters in order to elucidate the nature of the bonding in these compounds. The results can be summarized as follows.

Bare, ligand-free Ni clusters are in several aspects completely different from the carbonylated counterparts and, consequently, are expected to exhibit not only different physical properties but also a different chemical reactivity. In fact, consequences of carbonylation are as follows: The open-shell Ni 3d accepts charge from the valence 4s orbitals, which are destabilized by interaction with the CO ligands. This reduces the magnetic moment of the Ni atoms and, for coordinatively saturated clusters, results in diamagnetic compounds. The closed-shell Ni 3d orbitals hybridize with the Ni 4s4p orbitals and donate charge to CO, thus maintaining the Ni 3d population near 9. The energy gap between the highest filled and the lowest unoccupied MOs, which is rather small in free gas-phase Ni clusters, becomes substantial in the carbonylated forms, thus strongly reducing the metallic character of the metal atom framework. It has been suggested[48] that this gap decreases as the size of the cluster increases, with concomitant switch to a high-spin configuration beyond a critical cluster size.

The formation of the dianions is a favorable process because the extra electrons occupy "special" MOs with bonding character between the fragments, as in $[Ni_5(CO)_{12}]^{2-}$, or between the monomers, as in $[Ni_6(CO)_{12}]^{2-}$. It is worth noting that most probably the same mechanism contributes to the stabilization of higher oligomeric forms, such as the recently synthesized $[Ni_9(CO)_{18}]^{2-}$ compound,[46] consisting of three stacked $Ni_3(CO)_3(\mu\text{-}CO)_3$ layers.

These distinctive structural and electronic features lead to the conclusion that molecular ligand-covered metal clusters cannot be simply regarded as small pieces of metals surrounded by ligands. The fact that, in several cases, the metal atom framework of a cluster assumes a closed-packed geometry typical of bulk metals does not itself imply that the clusters are emulating the metals. Actually, they are not, at least in the case of Ni, as indicated by the different metal–metal interactions in the carbonylated forms, shown, for instance, by the electron density contour plots.

The analogy between molecular clusters and surfaces is more apparent than substantial for these cluster compounds. Because of the high number of ligands per metal atom, the bonding in molecular clusters can be better described in molecular terms, with localized bond pairs rather than with very delocalized multicenter bonds as in free metal clusters.[41] In order to approach a metallic regime, the cluster must lose part of its ligands by thermal or photochemical treatment or the size of the cluster must be increased so that the number of uncoordinated metal atoms equals or exceeds that of the CO-bonded metal atoms.

Acknowledgment. We thank Dr. R. Della Pergola, University of Milan, for recording and making available the optical spectrum of the $[Ni_6(CO)_{12}]^{2-}$ cluster. Further, we acknowledge the assistance of J.-P. Kubenka, G. Drechsler, Th. Fox, and P. Knappe, TU München. This work was supported by the Deutsche Forschungsgemeinschaft through Sonderforschungsbereich 128 and 338, which also made possible the stay of G.P. at the TU München, and by the Fonds der Chemischen Industrie.

(44) For instance: (a) Hermann, K.; Bagus, P. S. *Phys. Rev. B* **1977**, *16*, 4195. (b) Pacchioni, G.; Koutecký, J. *J. Phys. Chem.* **1987**, *91*, 2658. (c) Bauschlicher, C. W. *J. Chem. Phys.* **1986**, *84*, 250. (d) Panas, I.; Siegbahn, P.; Wahlgren, U. *Theor. Chim. Acta* **1988**, *74*, 167.

(45) Whitten, J. L.; Pakkanen, T. A. *Phys. Rev. B* **1980**, *21*, 4357.

(46) Nagaki, D. A.; Lower, L. D.; Longoni, G.; Chini, P.; Dahl, L. *Organometallics* **1986**, *5*, 1764.